Korean J Physiol Pharmacol 2021;25(4):355-363
https://doi.org/10.4196/kjpp.2021.25.4.355

KJPP

Original Article

Deletion of adipose triglyceride lipase abolishes blood flow increase after β3-adrenergic stimulation in visceral adipose tissue of mice

Hye-Jin Lee[1,2], Bo-Yeong Jin[1,2], Mi-Rae Park[1,2], Kwan Sik Seo[3], Yong Taek Jeong[1,2], Sang-Hyun Choi[1], and Dong-Hoon Kim[1,2,*]

[1]*Department of Pharmacology, Korea University College of Medicine,* [2]*BK21 Graduate Program, Department of Biomedical Sciences, Korea University College of Medicine, Seoul 02841,* [3]*Department of Rehabilitation Medicine, Seoul National University Hospital, Seoul 03080, Korea*

ARTICLE INFO

Received January 23, 2021
Revised March 22, 2021
Accepted March 23, 2021

***Correspondence**
Dong-Hoon Kim
E-mail: LDHKIM@korea.ac.kr

Key Words
Adipose tissue blood flow
Adipose triglyceride lipase
Beta adrenergic receptors
Lipolysis
Vasculature

ABSTRACT Dynamic changes in adipose tissue blood flow (ATBF) with nutritional status play a role in the regulation of metabolic and endocrine functions. Activation of the sympathetic nervous system *via* β-adrenergic receptors (β-AR) contributes to the control of postprandial enhancement of ATBF. Herein, we sought to identify the role of each β-AR subtype in the regulation of ATBF in mice. We monitored the changes in visceral epididymal ATBF (VAT BF), induced by local infusion of dobutamine, salbutamol, and CL316,243 (a selective β1-, β2-, and β3-AR agonist, respectively) into VAT of lean CD-1 mice and global adipose triglyceride lipase (ATGL) knockout (KO) mice, using laser Doppler flowmetry. Administration of CL316,243, known to promote lipolysis in adipocytes, significantly increased VAT BF of CD-1 mice to a greater extent compared to that of the vehicle, whereas administration of dobutamine or salbutamol did not produce significant differences in VAT BF. The increase in VAT BF induced by β3-AR stimulation disappeared in ATGL KO mice as opposed to their wild-type (WT) littermates, implying a role of ATGL-mediated lipolysis in the regulation of VAT BF. Different vascular reactivities occurred despite no significant differences in vessel density and adiposity between the groups. Additionally, the expression levels of the angiogenesis-related genes were significantly higher in VAT of ATGL KO mice than in that of WT, implicating an association of ATBF responsiveness with angiogenic activity in VAT. Our findings suggest a potential role of β3-AR signaling in the regulation of VAT BF *via* ATGL-mediated lipolysis in mice.

INTRODUCTION

White adipose tissue (WAT) is highly vascularized, and WAT microcirculation plays an important role in regulating metabolic and endocrine functions by exchanging oxygen, nutrients, and wastes with adipocytes [1]. Inadequate perfusion in WAT was hypothesized to cause WAT malfunction including hypoxia, as well as angiogenesis and inflammation [2-5]. Indeed, adipose tissue blood flow (ATBF) is increased after oral glucose ingestion in lean healthy subjects, whereas the responsiveness of ATBF to nutritional stimuli is blunted in obese and insulin-resistant subjects [6-8]. Therefore, it is important to understand the underlying mechanism of vascular reactivity to develop a novel therapeutic strategy for treating obesity.

WAT is densely innervated by the sympathetic nervous system, and its activation is essential for lipolysis in WAT [9-11]. Activation of β-adrenergic receptor (β-AR) signaling mediates a postprandial increase in ATBF as well as lipolysis in the subcutaneous

Author contributions: H.J.L., B.Y.J., and M.R.P. conducted the experiments. H.J.L. and D.H.K. designed the study, analyzed the data, and wrote the manuscript. B.Y.J., K.S.S., Y.T.J., and S.H.C. provided critical comments and contributed to the interpretation of this study. All authors discussed the results and contributed to the final manuscript.

adipose tissue (SAT) of humans [12-16]. β-ARs are a class of G protein-coupled receptors that are classified into three subtypes: β1-AR, β2-AR, and β3-AR. Each β-AR participates in various functions including regulation of heart rate, smooth muscle relaxation, and lipolysis [17,18]. Despite the diverse actions of each β-AR subtype, the exact role of each β-AR subtype in regulating ATBF in WAT remains unclear.

WAT is characterized as SAT and visceral adipose tissue (VAT) based on the anatomical sites and has depot-specific characteristics such as adipokine secretion, lipolysis, inflammation, and angiogenesis [19]. Increased VAT mass is strongly associated with the occurrence of metabolic syndrome, including cardiovascular disease and type 2 diabetes compared to SAT mass. Despite the important role of VAT in metabolic processes, studies on vascular reactivity in VAT have received less attention [14,20-24]. It is required to understand the mechanisms underlying the regulation of VAT BF in the development of obesity.

In this study, we sought to identify the effect of each β-AR subtype on vascular reactivity in VAT of mice *via* monitoring changes in blood flow during local infusion of each β-AR subtype agonist using laser Doppler flowmetry. Additionally, we sought to investigate the association of β3-AR stimulation-induced alteration in VAT BF with lipolysis using global adipose triglyceride lipase (ATGL) knockout (KO) mice. Furthermore, we sought to provide evidence for the relationship between lipolysis and angiogenesis in VAT of ATGL KO mice. This study suggests that β3-AR activation plays an important role in the control of vascular reactivity, presumably *via* ATGL-mediated lipolysis in VAT of mice.

METHODS

Animals

All experimental mice were maintained individually in standard mouse cages with a 12 h light/dark cycle in an environmentally controlled room (humidity 50% ± 10%, temperature 22°C ± 2°C) and had *ad libitum* access to water and regular chow diet (5L79 diet; LabDiet, St. Louis, MO, USA). A total of 43 of seven-week-old male CD-1 mice were obtained from Orient Bio (Seongnam, Korea) to investigate the effect of the β-adrenergic receptor (β-AR) subtype-selective stimulation on changes in visceral epididymal adipose tissue blood flow (VAT BF). After one week of acclimatization, the mice were randomly divided into three groups to monitor changes in VAT BF during local infusion of selective β1-AR agonist (dobutamine, D0676; Sigma-Aldrich, St Louis, MO, USA), selective β2-AR agonist (salbutamol, S8260; Sigma-Aldrich), and selective β3-AR agonist (CL316,243, C5976; Sigma-Aldrich) into VAT.

To identify the role of lipolysis induced by β3-AR subtype stimulation in the regulation of VAT BF, we compared changes in VAT BF during local infusion of the β3-AR agonist, CL316,243, into VAT of male global ATGL KO mice and wild-type (WT) littermate mice. Global ATGL KO mice were generated by breeding heterozygous ATGL mice on a C57BL/6 background. Ten-week-old homozygous male ATGL KO mice and their WT littermates were used for this study. All experiments were performed under fed conditions. All experimental procedures followed the guidelines for the ethical use of animals, issued by the Institutional Animal Care and Use Committee of Korea University, and were

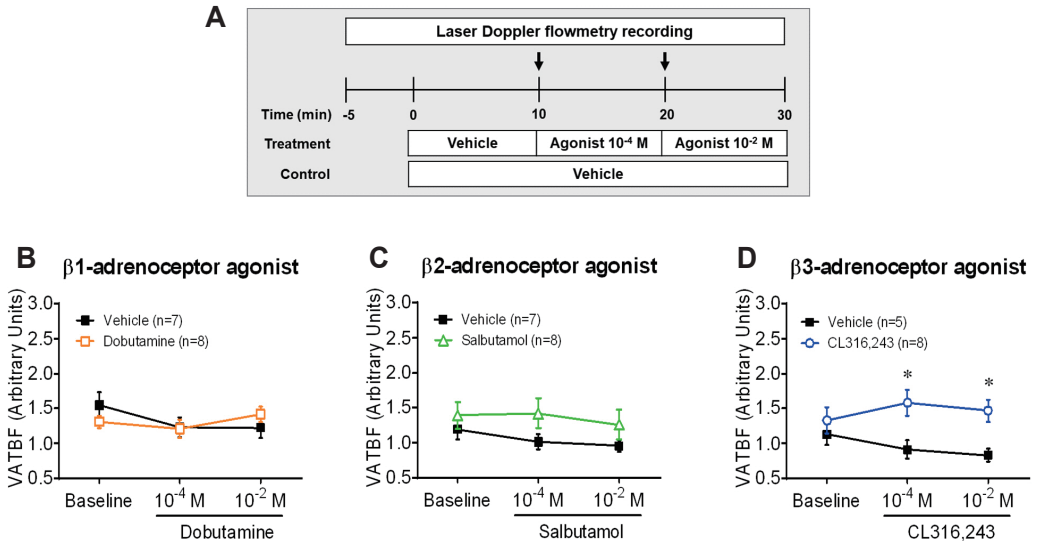

Fig. 1. Effects of β-adrenergic receptor subtypes on the regulation of visceral adipose tissue blood flow (VAT BF) in CD-1 mice. (A) Experimental timeline diagram. After stabilizing VAT BF for 5 min, vehicle and agonists (10^{-4} and 10^{-2} M) were infused into VAT a rate of 0.5 μl min^{-1} for 10 min, respectively. Arrows represent the time point of the switch in the agonist delivery. (B) Changes in VAT BF induced by stimulation of dobutamine, a selective β1-adrenergic receptor agonist. (C) Changes in VAT BF induced by stimulation of salbutamol, a selective β2-adrenergic receptor agonist. (D) Changes in VAT BF induced by stimulation of CL316,243, a selective β3-adrenergic receptor agonist. *p < 0.05.

approved by the same committee.

VAT BF measurement using laser Doppler flowmetry

Mice were anesthetized using an intraperitoneal injection of ketamine/xylazine mixture (ketamine: 115 mg/kg body weight, ketamine hydrochloride, Yuhan, Seoul, Korea; Rompun: 17 mg/kg body weight, xylazine hydrochloride, Bayer Korea, Seoul, Korea). During the VAT BF experiment, a rectal temperature probe was inserted into mice and placed on a heating pad to maintain body temperature at 36.5°C. The flow probe of a laser Doppler flowmeter (Type N18 and BLF22; Transonic Systems Inc., Ithaca, NY, USA) was placed on the surface of VAT, and the changes in VAT BF were recorded at the same site during the experiment. From time point zero, vehicle (normal saline) or each agonist was delivered sequentially into VAT at a rate of 0.5 μl min^{-1} for 10 min using a customized injector adjacent to the flow probe. Changes in VAT BF by local infusion of each selective β-AR agonist were performed as dose-response (10^{-4} and 10^{-2} M) experiments in male CD-1 mice (Fig. 1A). The effect of selective β3-AR agonist CL316,243 on the alteration of VAT BF in ATGL KO mice was tested by local infusion at a concentration of 10^{-2} M (Fig. 3E). The analog signals were digitized and displayed using a data processing program. The average rate of tissue perfusion (arbitrary units) was recorded using a data analysis LabScribe2 software (iWorx Systems Inc., Dover, NH, USA).

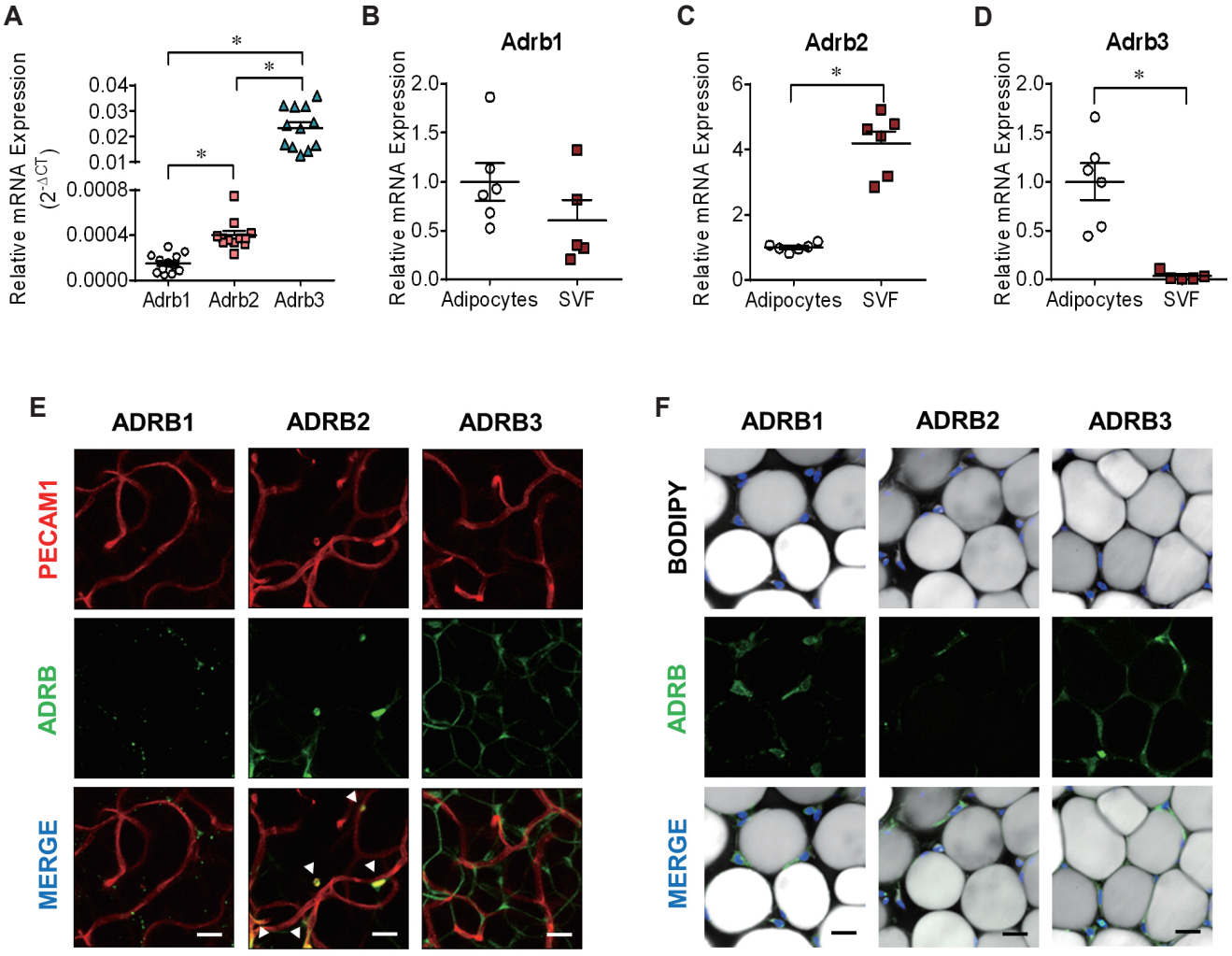

Fig. 2. Distribution and colocalization of β-adrenergic receptor subtypes in visceral epididymal fat (VAT) of mice. (A) Comparison of the expression levels of *Adrb1*, *Adrb2*, and *Adrb3* in VAT of CD-1 male mice fed a normal chow diet at 8 weeks of age. The ΔCt method ($2^{-\Delta Ct}$) was used to calculate the relative expression level of each gene. (B–D) Comparison of the expression levels of *Adrb1* (B), *Adrb2* (C), and *Adrb3* (D) between fractionated adipocytes and stromal vascular fraction (SVF) in VAT of C57BL/6N male mice fed a normal chow diet at 9 weeks of age. The relative mRNA expression was calculated using the ΔΔCt method ($2^{-\Delta\Delta Ct}$). (E, F) Representative images of double immunofluoresnce staining of whole-mount VAT using ADRB1, ADRB2, or ADRB3 antibodies with PECAM1 antibodies (E) or BODIPY (F) dye in C57BL/6N male mouse fed a normal chow diet at 8 weeks of age. White arrowheads indicate localization of ADRB2 in PECAM1+ vessels. Images are shown at a magnification of ×500. Scale bars, 20 μm. *$p < 0.05$.

Body composition analysis

Body fat and lean mass were measured using a nuclear magnetic resonance spectrometer (LF90 Minispec; Bruker Optics, The Woodlands, TX, USA).

Quantitative RT-PCR

Total RNA was extracted from VAT using TRIzol reagent (Invitrogen, Carlsbad, CA, USA), and cDNA was synthesized using iScript cDNA synthesis kit (Bio-Rad, Hercules, CA, USA). The cDNA was mixed with relevant probes (Taqman Gene Expression Assays and TaqMan Gene Expression Master Mix; Applied Biosystems, Foster City, CA, USA). Real-time quantitative PCR was conducted using an ABI 7500 Real-Time PCR system (Applied Biosystems). Expression of each gene was normalized to the constitutively expressed *Rpl32* gene, and relative expression was quantified. The ΔCt values were obtained by performing the calculation Ct (a target gene) – Ct (a reference gene) in each sample. The ΔCt method ($2^{-\Delta Ct}$) was used to calculate the relative expression level of each gene (Fig. 2A). The ΔΔCt method ($2^{-\Delta\Delta Ct}$) was presented as the fold changes of gene expression in a target group (stromal vascular fraction or ATGL KO mice) relative to a reference group (adipocytes or WT mice), normalized to a reference gene. The relative gene expression was set to 1 for reference group (Figs. 2B–D, 4A, and 5F). Primers used for qRT-PCR are listed in Supplementary Table 1.

Western blot analyses

Total proteins of VAT were obtained by homogenizing using RIPA lysis buffer (Santa Cruz Biotechnology, Santa Cruz, CA, USA). Protein extracts were separated by electrophoresis and transferred to PVDF membrane. The membranes were blocked with 10% skim milk for 1 h, and then incubated overnight with primary antibodies diluted at a ratio of 1: 1000 for ADRB3 (ab94506; Abcam, Cambridge, MA, USA), ATGL (2138; CST, Beverly, MA, USA), p-HSL Ser563 (4139; CST), HSL (4107; CST) and β-actin (4967; CST) at 4°C. Corresponding secondary antibody was incubated for 2 h and the membrane were developed with PicoEPD western reagent (Elpis Biotech, Daejeon, Korea).

Histological analyses

Whole-mount immunofluorescence analyses were performed as described with minor modifications [25]. Whole-mount tissues were incubated with primary antibody against PECAM-1 (1:200 dilution, MAB1398Z; Millipore, Billerica, MA, USA), ADRB1 (1:200 dilution, PA1-049; Thermo Fisher Scientific, Waltham, MA, USA), ADRB2 (1:200 dilution, ab182136; Abcam), and ADRB3 (1:200 dilution) for 60 h at 4°C. After six washes of 20 min each, the tissues were incubated overnight with the species-specific secondary antibody. The stained whole-mount tissues were subsequently incubated with a fructose solution as an optical clearing agent to diminish the amount of light scattering. The adipocytes and nuclei in whole-mount VAT were stained with

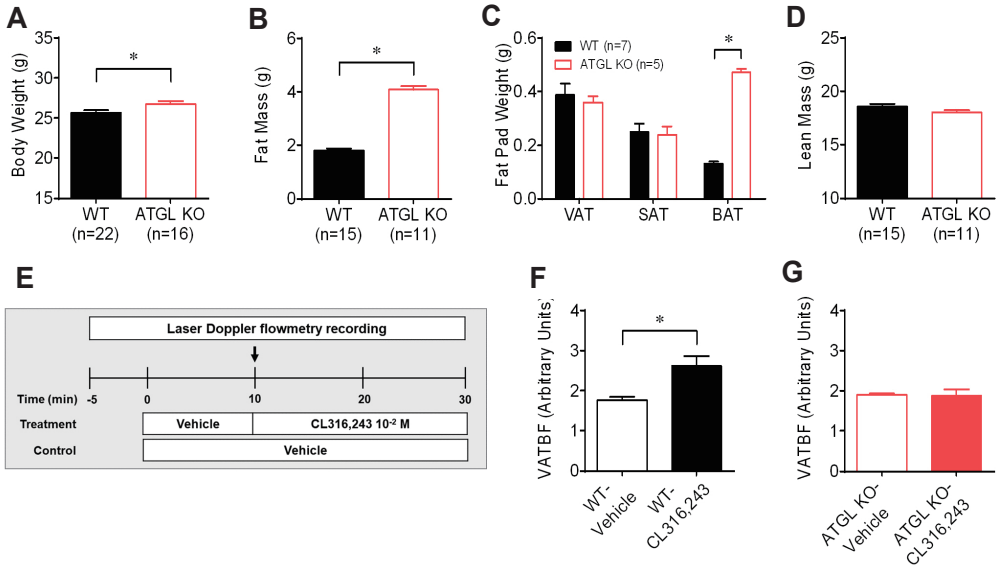

Fig. 3. Changes in visceral adipose tissue blood flow (VAT BF) to β3-adrenergic receptor stimulation in wild-type (WT) and adipose triglyceride lipase (ATGL) knockout (KO) mice. (A–D) Phenotype comparison of body weight (A), total fat mass (B), fat pad weights (C), and total lean mass (D) between WT and ATGL KO mice at 10 weeks of age. (E) Timeline diagram for the experiment on changes in VAT BF by stimulation of β3-adrenergic receptor agonist CL316,243. Arrows represent the time point of the switch in the agonist delivery. (F) Comparison of changes in VAT between the vehicle (n = 8) and CL316,243 (n = 8) infusion in WT mice at time point 30 min. (G) Comparison of changes in VAT between the vehicle (n = 4) and CL316,243 (n = 7) infusion in ATGL KO mice at time point 30 min. *p < 0.05.

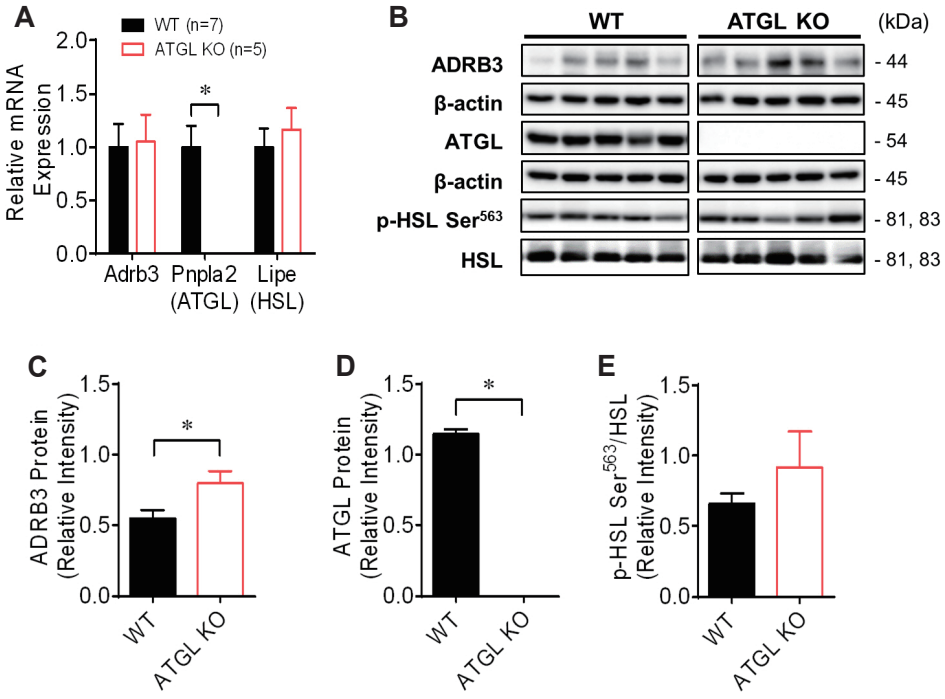

Fig. 4. Expression of β3-adrenergic receptor-mediated lipolysis associated mRNA and protein in visceral adipose tissue (VAT) of wild-type (WT) and adipose triglyceride lipase (ATGL) knockout (KO) mice. (A) Comparison of the gene expression of *Adrb3*, *Pnpla2*, and *Lipe* in VAT of WT and ATGL KO mice. The relative mRNA expression was calculated using the ΔΔCt method ($2^{-\Delta\Delta Ct}$). (B) Western blot analysis of lipolysis associated proteins, including ADRB3, ATGL, HSL, and p-HSL Ser^{563}. (C–E) The relative intensity of ADRB3 (C), ATGL (D), and phosphorylation of HSL on serine 563 (E). *Adrb3*, beta-3 adrenergic receptor; *Pnpla2*, Patatin Like Phospholipase Domain Containing 2 known as ATGL; *Lipe*, Lipase E, Hormone Sensitive Type known as hormone-sensitive lipase (HSL). *p < 0.05: WT (n = 7) *vs.* ATGL KO (n = 5) mice.

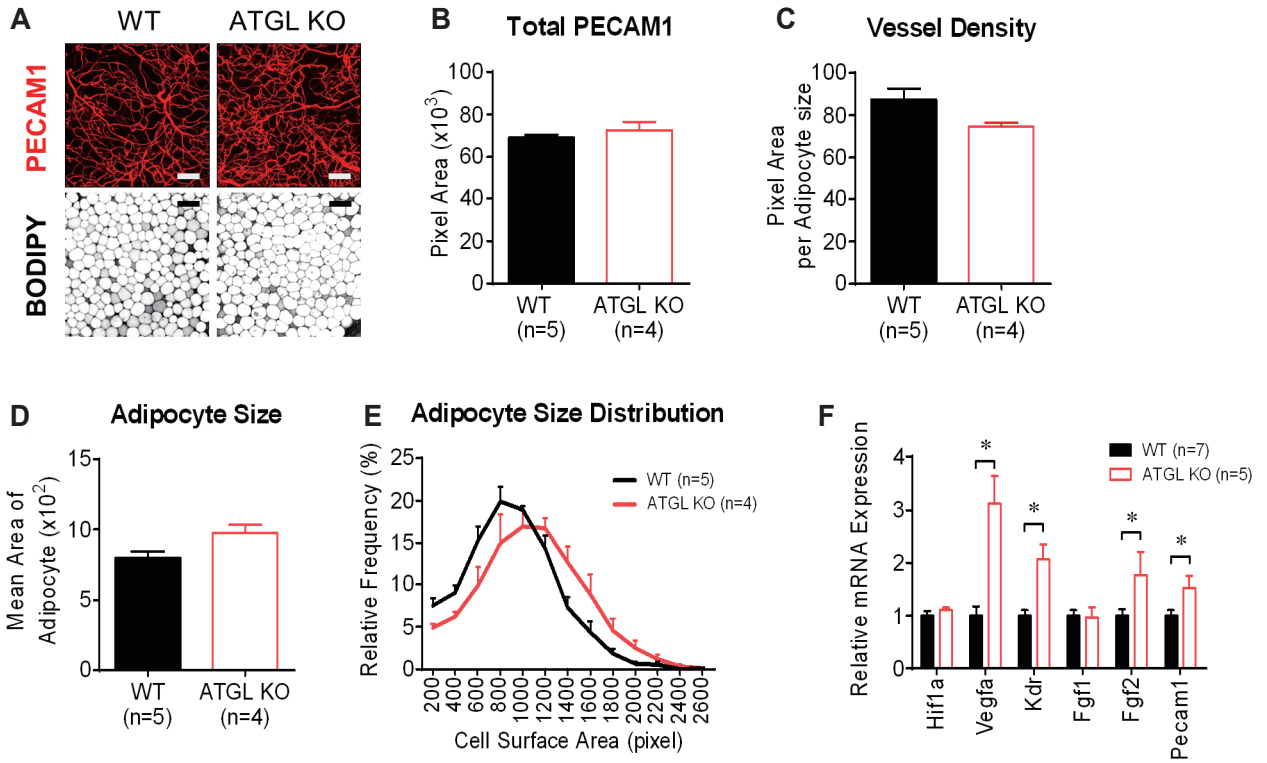

Fig. 5. Comparison of adipose tissue vessel morphology and angiogenesis-related mRNA expression in visceral adipose tissue (VAT) of wild-type (WT) and adipose triglyceride lipase (ATGL) knockout (KO) mice. (A) Representative images of vasculature and adipocytes of whole-mount VAT in WT and ATGL KO mice. Images are shown at a magnification of ×100. Scale bars, 100 μm. (B, C) Quantitative total vessel area (B) and vessel density normalized to average adipocyte size (C) between WT and ATGL KO mice. (D, E) Quantification of mean area of adipocyte (D) and distribution of adipocyte size (E) between WT and ATGL KO mice. (F) Comparison of the expression levels of genes related to angiogenesis in VAT of WT and ATGL KO mice. The relative mRNA expression was calculated using the ΔΔCt method ($2^{-\Delta\Delta Ct}$). *Hif1a*, hypoxia-inducible factor 1, alpha subunit; *Vegfa*, vascular endothelial growth factor A; *Kdr*, kinase insert domain protein receptor; *Fgf1*, fibroblast growth factor 1; *Fgf2*, fibroblast growth factor 2; *Pecam1*, platelet endothelial cell adhesion molecule 1. *p < 0.05.

BODIPY (1:1,000 dilution, D-3835; Invitrogen) and DAPI (1:1,000 dilution, D9542; Sigma-Aldrich). All images were captured under a confocal microscope (Zeiss confocal LSM 700 laser scanning microscope) at a magnification of ×100 or ×500.

Statistical analyses

Data were analyzed using GraphPad Prism 6.0 software (GraphPad Software Inc., San Diego, CA, USA) and expressed as mean ± standard error of the mean. Changes in VAT BF were analyzed using two-way ANOVA followed by Bonferroni's multiple comparison test. Student's t-test was performed for data analysis between ATGL KO mice and WT littermates. $p < 0.05$ was considered statistically significant.

RESULTS

Effect of local β-adrenergic receptor subtypes stimulation on VAT BF in mice

To identify the effect of each β-adrenergic receptor (β-AR) subtype on the regulation of visceral adipose tissue blood flow (VAT BF), we compared changes in VAT BF of CD-1 mice during local infusion of β1-, β2-, or β3-AR subtype-selective agonists into VAT. Local delivery of CL316,243, a selective β3-AR agonist, into VAT at a concentration of 10^{-4} M significantly increased VAT BF of CD-1 mice to a greater extent compared to that of the vehicle. However, local delivery of dobutamine, a selective β1-AR agonist, and salbutamol, a selective β2-AR agonist, into VAT did not alter VAT BF of CD-1 mice (Fig. 1B–D). These results suggest a selective role of β3-AR stimulation on VAT BF in mice.

Differential localization of β-adrenergic receptor subtypes in VAT of mice

To determine the expression of each β-AR subtype in VAT, we measured the expression levels of *Adrb1*, *Adrb2*, and *Adrb3* in VAT of CD-1 mice or C57BL/6N mice. All three β-AR subtypes were expressed in VAT of CD-1 and C57BL/6N mice. The expression level of *Adrb3* was higher than that of *Adrb1* and *Adrb2* in VAT of CD-1 mice (Fig. 2A). To better understand the distribution of each β-AR subtype in VAT, we compared the expression levels of *Adrb1*, *Adrb2*, and *Adrb3* in mature adipocytes and stromal vascular fraction (SVF) obtained from VAT of C57BL/6N mice or performed a colocalization study in VAT using endothelium or adipocytes markers. The expression level of *Adrb1* between the adipocyte and the SVF was similar. *Adrb2* was highly expressed in the SVF compared to the adipocytes. In contrast, *Adrb3* was highly expressed in the adipocyte compared to the SVF (Fig. 2B–D). Consistent with the differential distribution of each β-AR subtype, ADRB3 signals were mostly co-localized with the BODIPY+ adipocytes rather than the PECAM1+ vessels in VAT of the mice. In contrast, we detected co-localization of the ADRB2 with the PECAM1+ vessels. ADRB1 was expressed around the adipocyte nuclei, but rarely in the PECAM1+ vessels (Fig. 2E, F). These results indicated that the β3-AR subtypes were predominantly localized in adipocytes within VAT of the mice, implying a potential role of β3-AR-mediated lipolysis in the regulation of VAT BF.

Effect of local β3-adrenergic receptor subtype stimulation on VAT BF in global ATGL KO mice

To investigate the role of β3-AR-mediated lipolysis in the regulation of VAT BF, we compared changes in VAT BF between ATGL KO and WT littermate mice at 10 weeks of age during local infusion of CL316,243 into VAT. ATGL, a target of β3-AR signaling, catalyzes the first step in the hydrolysis of triglycerides [26,27]. Body weight and total fat mass were significantly higher in ATGL KO mice than in WT mice (Fig. 3A, B). The increase in total fat mass was mainly because of brown adipose tissue mass rather than WAT including visceral epididymal and subcutaneous inguinal adipose tissue (VAT and SAT) at the age of 10 weeks (Fig. 3C). However, no significant difference in lean mass was observed between WT and ATGL KO mice (Fig. 3D). Consistent with the changes observed in VAT BF of CD-1 mice, local infusion of CL316,243 into VAT significantly increased VAT BF of WT mice to a greater extent compared to that of the vehicle (Fig. 3F). However, the infusion of CL316,243 into VAT did not enhance VAT BF in ATGL KO mice (Fig. 3G). These results suggest that changes in VAT BF induced by stimulation of the β3-AR subtype might be regulated *via* ATGL-mediated lipolysis.

Effect of absence of ATGL on β-adrenergic receptor-mediated lipolysis pathway

To investigate whether the absence of ATGL affects other signaling molecules related to the β-adrenergic receptor-mediated lipolysis pathway, we compared the expression levels of genes and proteins associated with lipolysis in VAT between WT and ATGL KO mice at 10 weeks of age. We confirmed the absence of ATGL gene and protein expression in VAT of ATGL KO mice (Fig. 4A, B, and D). The expression level of ADRB3 protein was higher in VAT of ATGL KO mice than in that of WT mice, although that of *Adrb3* was not different between WT and ATGL KO mice, presumably indicating a compensatory upregulation in ADRB3 expression (Fig. 4A–C). However, the expression levels of *Lipe*, encoding HSL, an enzyme that catalyzes the hydrolysis of diacylglycerol to monoacylglycerol, and the phosphorylated HSL on serine^{563}, measured as the ratio of p-HSL Ser^{563}:HSL, were not significantly different between WT and ATGL KO mice (Fig. 4A, B, and E). The results indicated that the absence of ATGL did not cause a compensatory increase in HSL activity, presum-

ably not affecting the deficiency of lipolysis in VAT of ATGL KO mice. Therefore, these findings suggest that the absence of ATGL-mediated lipolysis contributes to the lower vascular reactivity in VAT of ATGL KO mice.

Effect of absence of ATGL-mediated lipolysis on angiogenic activity in VAT

To investigate the association of impaired VAT vascular reactivity with VAT morphology in ATGL KO mice, we compared vessel density and adipocyte size in VAT between WT and ATGL KO mice (Fig. 5A). We found no significant differences in vessel density in VAT between WT and ATGL KO mice (Fig. 5B, C). The average size of VAT adipocytes was not significantly different between the groups. However, the fraction of bigger adipocytes tended to be higher and that of smaller adipocytes was lower in the VAT of ATGL KO mice than in VAT of WT mice (Fig. 5D, E).

Inadequate tissue perfusion results in less oxygen diffusion and increases the demand for tissue remodeling, including angiogenesis [2,5,28,29]. To determine whether impaired vascular reactivity promotes angiogenic activity in VAT, we compared the expression levels of angiogenesis-related genes in VAT between WT and ATGL KO mice. Consistent with the lower vascular reactivity in VAT of ATGL KO mice than in the VAT of WT mice, the expression levels of angiogenesis-related genes including *Vegfa*, *Kdr*, *Fgf2*, and *Pecam1* were markedly higher in VAT of ATGL KO mice than in that of WT mice (Fig. 5F). These results suggest that the absence of ATGL-mediated lipolysis promotes angiogenesis in VAT, presumably by lowering VAT vascular reactivity.

DISCUSSION

The aim of this study was to identify the role of β-AR subtypes in the regulation of adipose tissue blood flow (ATBF) in mice. β-AR stimulation contributes to the postprandial enhancement of ATBF, which is hypothesized to regulate functional metabolism by exchanging nutrients and wastes from adipocytes [1,12]. Given the role of ATBF in the maintenance of adipose tissue function, it was important to identify the mechanisms underlying the regulation of ATBF to develop novel strategeis for treating obesity [2,3,5,29,30]. In this study, we showed that only β3-AR participated in the enhancement of VAT BF in mice, which might be associated with ATGL-mediated lipolysis.

To identify the involvement of each β-AR subtype with the regulation of ATBF in mice, we used each β-AR subtype-selective agonist in separate experiments to evaluate the responsiveness of vascular reactivity in VAT of mice. We, for the first time, showed that only stimulation of β3-AR by CL316,243, a β3-AR-selective agonist, increased VAT BF in mice. Three β-AR subtypes coexist in various tissues, such as the heart, adipose tissue, lung, bladder, and uterus. Notably, β1-AR, expressed in the heart, contributes to myocardial contractility. β2-AR, abundantly located in the airway and vascular smooth muscles, involves vasorelaxation. β3-AR, predominantly expressed in the adipose tissue, is the major receptor that mediates lipolysis [31]. In this study, we detected the expression of all three β-AR subtypes in VAT of mice. Additionally, we showed that β3-AR were mainly expressed in adipocytes within VAT of mice while β2-AR in endothelium. Given the unique actions of each β-AR subtype, it was surprising that only β3-AR was involved in the regulation of ATBF, implying a role of β3-AR-associated lipolysis in the β-AR-mediated enhancement of ATBF (Figs. 1 and 2) [15,16].

Next, we investigated whether β3-AR-mediated lipolysis contributed to the β3-AR stimulation-induced increase in VAT BF in mice. To test this hypothesis, we compared changes in VAT BF during the infusion of CL316,243 between WT and ATGL KO mice. We found that the β3-AR stimulation-induced increase in VAT BF was negated in ATGL KO mice, while it was consistently observed in WT mice (Fig. 3). Additionally, we confirmed that

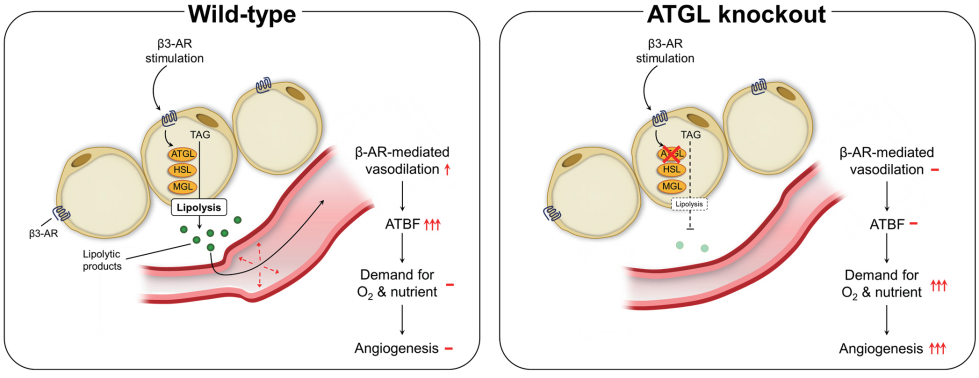

Fig. 6. Schematic diagram of the role of β3-adrenergic receptor-mediated lipolysis in the regulation of visceral adipose tissue blood flow. β3-adrenergic receptor (AR) signaling contributes to β-AR-mediated enhancement of visceral adipose tissue blood flow (VAT BF) in mice. Adipose triglyceride lipase (ATGL) deficiency negates the enhancement of VAT BF induced by β3-AR stimulation, suggesting the role of ATGL-mediated lipolysis in the regulation of VAT BF. This process may contribute to VAT remodeling in the development of obesity. TAG, triacylglycerol; HSL, hormone-sensitive lipase; MGL, monoglyceride lipase.

the absence of ATGL did not affect the activity of HSL, another key enzyme for lipolysis, in ATGL KO mice, implicating the exclusion of the possibility of a compensatory increase in lipolysis (Fig. 4). Thus, the results indicated a potential role of ATGL-mediated lipolysis in β3-AR stimulation-induced increase in VAT BF. In humans, the level of plasma norepinephrine in response to meal intake positively correlates with vascular reactivity in adipose tissue [7]. The postprandial enhancement of subcutaneous ATBF is lower in obese humans than in lean subjects; further, catecholamine-induced lipolysis is markedly lower in obese individuals [32,33]. Therefore, these studies support the link between lipolysis and vascular reactivity in this study.

In accordance with previous studies [34,35], we observed that global ATGL KO mice had greater body weight and total fat mass than WT mice, owing to the excessive lipid accumulation in the brown adipose tissue and heart of the former group. However, we did not observe significant differences in VAT and SAT masses between the two groups at 10 weeks of age (Fig. 3). Consistently, the average size of adipocytes and vessel density in VAT were not significantly different between WT and ATGL KO mice.

Given the effect of capillarization on ATBF in obesity [3,14,36,37], it is worth emphasizing that the difference in vascular reactivity in response to β3-AR stimulation occurs independently of the capillarization in the mice. Furthermore, we found that the expression levels of angiogenesis-related genes including *Vegfa*, *Kdr*, *Fgf2*, and *Pecam1* were higher in the VAT of ATGL KO mice than in that of WT mice (Fig. 5). The responsiveness of ATBF is closely associated with the occurrence of angiogenesis in WAT [3]. Therefore, the low vascular reactivity due to the absence of ATGL-mediated lipolysis might increase angiogenic activity enough to meet the demand for oxygen and nutrients in the VAT of ATGL KO mice (Fig. 6).

In conclusion, our findings indicate that VAT β3-AR signaling might play an important role in regulating VAT BF *via* ATGL-mediated lipolysis in mice. Further studies on the role of AT vascular reactivity *via* lipolysis in the development of obesity are required to help develop new strategies for a therapeutic approach to obesity.

ACKNOWLEDGEMENTS

This work was supported by the National Research Foundation of Korea (NRF) grant funded by the Ministry of Education (grant number 2017R1D1A1B03031216); the Ministry of Science & ICT (grant number 2015M3A9E7029172 & 2018R1A2B6001296); and a Korea University grant.

CONFLICTS OF INTEREST

The authors declare no conflicts of interest.

SUPPLEMENTARY MATERIALS

Supplementary data including one table can be found with this article online at https://doi.org/10.4196/kjpp.2021.25.4.355.

REFERENCES

1. Cao Y. Adipose tissue angiogenesis as a therapeutic target for obesity and metabolic diseases. *Nat Rev Drug Discov.* 2010;9:107-115.
2. Goossens GH, Bizzarri A, Venteclef N, Essers Y, Cleutjens JP, Konings E, Jocken JW, Cajlakovic M, Ribitsch V, Clément K, Blaak EE. Increased adipose tissue oxygen tension in obese compared with lean men is accompanied by insulin resistance, impaired adipose tissue capillarization, and inflammation. *Circulation.* 2011;124:67-76.
3. Ye J. Emerging role of adipose tissue hypoxia in obesity and insulin resistance. *Int J Obes (Lond).* 2009;33:54-66.
4. Unamuno X, Gómez-Ambrosi J, Rodríguez A, Becerril S, Frühbeck G, Catalán V. Adipokine dysregulation and adipose tissue inflammation in human obesity. *Eur J Clin Invest.* 2018;48:e12997.
5. Ye J, Gao Z, Yin J, He Q. Hypoxia is a potential risk factor for chronic inflammation and adiponectin reduction in adipose tissue of ob/ob and dietary obese mice. *Am J Physiol Endocrinol Metab.* 2007;293:E1118-E1128.
6. Dimitriadis G, Lambadiari V, Mitrou P, Maratou E, Boutati E, Panagiotakos DB, Economopoulos T, Raptis SA. Impaired postprandial blood flow in adipose tissue may be an early marker of insulin resistance in type 2 diabetes. *Diabetes Care.* 2007;30:3128-3130.
7. Karpe F, Fielding BA, Ilic V, Macdonald IA, Summers LK, Frayn KN. Impaired postprandial adipose tissue blood flow response is related to aspects of insulin sensitivity. *Diabetes.* 2002;51:2467-2473.
8. McQuaid SE, Hodson L, Neville MJ, Dennis AL, Cheeseman J, Humphreys SM, Ruge T, Gilbert M, Fielding BA, Frayn KN, Karpe F. Downregulation of adipose tissue fatty acid trafficking in obesity: a driver for ectopic fat deposition? *Diabetes.* 2011;60:47-55.
9. Bartness TJ, Liu Y, Shrestha YB, Ryu V. Neural innervation of white adipose tissue and the control of lipolysis. *Front Neuroendocrinol.* 2014;35:473-493.
10. Bowers RR, Festuccia WT, Song CK, Shi H, Migliorini RH, Bartness TJ. Sympathetic innervation of white adipose tissue and its regulation of fat cell number. *Am J Physiol Regul Integr Comp Physiol.* 2004;286:R1167-R1175.
11. Cao Y, Wang H, Wang Q, Han X, Zeng W. Three-dimensional volume fluorescence-imaging of vascular plasticity in adipose tissues. *Mol Metab.* 2018;14:71-81.
12. Ardilouze JL, Fielding BA, Currie JM, Frayn KN, Karpe F. Nitric oxide and beta-adrenergic stimulation are major regulators of preprandial and postprandial subcutaneous adipose tissue blood flow in humans. *Circulation.* 2004;109:47-52.
13. Sotornik R, Brassard P, Martin E, Yale P, Carpentier AC, Ardilouze JL. Update on adipose tissue blood flow regulation. *Am J Physiol Endocrinol Metab.* 2012;302:E1157-E1170.
14. Frayn KN, Karpe F. Regulation of human subcutaneous adipose tissue blood flow. *Int J Obes (Lond).* 2014;38:1019-1026.
15. Collins S. β-adrenoceptor signaling networks in adipocytes for recruiting stored fat and energy expenditure. *Front Endocrinol (Laus-*

anne). 2012;2:102.
16. Evans BA, Merlin J, Bengtsson T, Hutchinson DS. Adrenoceptors in white, brown, and brite adipocytes. *Br J Pharmacol.* 2019;176:2416-2432.
17. Tanaka Y, Horinouchi T, Koike K. New insights into beta-adrenoceptors in smooth muscle: distribution of receptor subtypes and molecular mechanisms triggering muscle relaxation. *Clin Exp Pharmacol Physiol.* 2005;32:503-514.
18. Balligand JL. Cardiac salvage by tweaking with beta-3-adrenergic receptors. *Cardiovasc Res.* 2016;111:128-133.
19. Ibrahim MM. Subcutaneous and visceral adipose tissue: structural and functional differences. *Obes Rev.* 2010;11:11-18.
20. Ledoux S, Queguiner I, Msika S, Calderari S, Rufat P, Gasc JM, Corvol P, Larger E. Angiogenesis associated with visceral and subcutaneous adipose tissue in severe human obesity. *Diabetes.* 2008;57:3247-3257.
21. Farb MG, Gokce N. Visceral adiposopathy: a vascular perspective. *Horm Mol Biol Clin Investig.* 2015;21:125-136.
22. Shah RV, Murthy VL, Abbasi SA, Blankstein R, Kwong RY, Goldfine AB, Jerosch-Herold M, Lima JA, Ding J, Allison MA. Visceral adiposity and the risk of metabolic syndrome across body mass index: the MESA Study. *JACC Cardiovasc Imaging.* 2014;7:1221-1235.
23. Després JP, Lemieux I. Abdominal obesity and metabolic syndrome. *Nature.* 2006;444:881-887.
24. Kwon H, Kim D, Kim JS. Body fat distribution and the risk of incident metabolic syndrome: a longitudinal cohort study. *Sci Rep.* 2017;7:10955.
25. Xue Y, Lim S, Bråkenhielm E, Cao Y. Adipose angiogenesis: quantitative methods to study microvessel growth, regression and remodeling in vivo. *Nat Protoc.* 2010;5:912-920.
26. Bolsoni-Lopes A, Alonso-Vale MI. Lipolysis and lipases in white adipose tissue- an update. *Arch Endocrinol Metab.* 2015;59:335-342.
27. Zechner R, Zimmermann R, Eichmann TO, Kohlwein SD, Haemmerle G, Lass A, Madeo F. FAT SIGNALS--lipases and lipolysis in lipid metabolism and signaling. *Cell Metab.* 2012;15:279-291.
28. Kabon B, Nagele A, Reddy D, Eagon C, Fleshman JW, Sessler DI, Kurz A. Obesity decreases perioperative tissue oxygenation. *Anesthesiology.* 2004;100:274-280.
29. Pasarica M, Sereda OR, Redman LM, Albarado DC, Hymel DT, Roan LE, Rood JC, Burk DH, Smith SR. Reduced adipose tissue oxygenation in human obesity: evidence for rarefaction, macrophage chemotaxis, and inflammation without an angiogenic response. *Diabetes.* 2009;58:718-725.
30. He Q, Gao Z, Yin J, Zhang J, Yun Z, Ye J. Regulation of HIF-1{alpha} activity in adipose tissue by obesity-associated factors: adipogenesis, insulin, and hypoxia. *Am J Physiol Endocrinol Metab.* 2011;300:E877-E885.
31. Perrone MG, Notarnicola M, Caruso MG, Tutino V, Scilimati A. Upregulation of beta3-adrenergic receptor mRNA in human colon cancer: a preliminary study. *Oncology.* 2008;75:224-229.
32. Langin D, Dicker A, Tavernier G, Hoffstedt J, Mairal A, Rydén M, Arner E, Sicard A, Jenkins CM, Viguerie N, van Harmelen V, Gross RW, Holm C, Arner P. Adipocyte lipases and defect of lipolysis in human obesity. *Diabetes.* 2005;54:3190-3197.
33. Flores-Opazo M, Trieu J, Naim T, Valladares-Ide D, Zbinden-Foncea H, Stapleton D. Defective fasting-induced PKA activation impairs adipose tissue glycogen degradation in obese Zucker rats. *Int J Obes (Lond).* 2020;44:500-509.
34. Haemmerle G, Moustafa T, Woelkart G, Büttner S, Schmidt A, van de Weijer T, Hesselink M, Jaeger D, Kienesberger PC, Zierler K, Schreiber R, Eichmann T, Kolb D, Kotzbeck P, Schweiger M, Kumari M, Eder S, Schoiswohl G, Wongsiriroj N, Pollak NM, *et al.* ATGL-mediated fat catabolism regulates cardiac mitochondrial function via PPAR-α and PGC-1. *Nat Med.* 2011;17:1076-1085.
35. Haemmerle G, Lass A, Zimmermann R, Gorkiewicz G, Meyer C, Rozman J, Heldmaier G, Maier R, Theussl C, Eder S, Kratky D, Wagner EF, Klingenspor M, Hoefler G, Zechner R. Defective lipolysis and altered energy metabolism in mice lacking adipose triglyceride lipase. *Science.* 2006;312:734-737.
36. Onogi Y, Wada T, Kamiya C, Inata K, Matsuzawa T, Inaba Y, Kimura K, Inoue H, Yamamoto S, Ishii Y, Koya D, Tsuneki H, Sasahara M, Sasaoka T. PDGFRβ regulates adipose tissue expansion and glucose metabolism via vascular remodeling in diet-induced obesity. *Diabetes.* 2017;66:1008-1021.
37. Song MG, Lee HJ, Jin BY, Gutierrez-Aguilar R, Shin KH, Choi SH, Um SH, Kim DH. Depot-specific differences in angiogenic capacity of adipose tissue in differential susceptibility to diet-induced obesity. *Mol Metab.* 2016;5:1113-1120.